

Circulation Research

JOURNAL OF THE AMERICAN HEART ASSOCIATION



Effect of arterial impedance changes on the end-systolic pressure- volume relation

WL Maughan, K Sunagawa, D Burkhoff and K Sagawa

Circ. Res. 1984;54;595-602

Circulation Research is published by the American Heart Association, 7272 Greenville Avenue, Dallas, TX 75214

Copyright © 1984 American Heart Association. All rights reserved. Print ISSN: 0009-7330. Online ISSN: 1524-4571

The online version of this article, along with updated information and services, is located on the World Wide Web at:

<http://circres.ahajournals.org>

Subscriptions: Information about subscribing to Circulation Research is online at
<http://circres.ahajournals.org/subscriptions/>

Permissions: Permissions & Rights Desk, Lippincott Williams & Wilkins, a division of Wolters Kluwer Health, 351 West Camden Street, Baltimore, MD 21202-2436. Phone: 410-528-4050. Fax: 410-528-8550. E-mail:
journalpermissions@lww.com

Reprints: Information about reprints can be found online at
<http://www.lww.com/reprints>

Effect of Arterial Impedance Changes on the End-Systolic Pressure-Volume Relation

W.L. Maughan, K. Sunagawa, D. Burkhoff, and K. Sagawa

From The Johns Hopkins Medical Institutions, Cardiology Division, Department of Medicine, and Department of Biomedical Engineering, Baltimore, Maryland

SUMMARY. To study the end-systolic pressure-volume relationship of left ventricle ejection against physiological afterload, we imposed seven simulated arterial impedances on excised canine left ventricles connected to a newly developed servo-pump system. We set each of the impedance parameters (resistance, capacitance, and characteristic impedance) to 50, 100, and 200% of normal value (resistance: 3 mm Hg sec/ml; capacitance: 0.4 ml/mm Hg; characteristic impedance: 0.2 mm Hg sec/ml), while leaving the other parameters normal. Under a given impedance, the end-systolic pressure-volume relationship was determined by preloading the ventricle at four different end-diastolic volumes. There was no significant change in the slope of the end-systolic pressure-volume relationship with changes in any of the afterloading impedance parameters. However, the volume intercept of the end-systolic pressure-volume relationship decreased significantly with resistance from 5.5 ± 1.0 (SE) ml at resistance equal to 1.5 mm Hg sec/ml to 0.6 ± 1.8 ml at resistance equal to 6 mm Hg sec/ml ($P < 0.01$). The volume axis intercept also decreased with characteristic impedance, from 5.9 ± 2.0 ml at a characteristic impedance of 0.1 mm Hg sec/ml to 5.4 ± 2.1 ml at a characteristic impedance of 0.4 mm Hg sec/ml, ($P < 0.05$). We conclude that the slope of the end-systolic pressure-volume relationship is insensitive to a wide range of changes in afterload impedance, but its volume intercept is dependent on resistance and characteristic impedance. (*Circ Res* 54: 595-602, 1984)

OVER the past 10 years, the use of the end-systolic pressure-volume relationship (ESPVR) as a measure of ventricular pump function has gained increased acceptance. The salient features of this relationship are its insensitivity of left ventricular filling (preload) and incorporation of afterload pressure into its measurements (Sagawa et al., 1977; Sagawa, 1981). Although other features of the ESPVR, such as the linearity of this relationship and its sensitivity to changes in inotropic background, have been confirmed by other investigators (Marsh et al., 1979; Mehmehl et al., 1981; Nivatpumin et al., 1979), most of the evidence for load independence has been based on those data obtained from ventricles contracting under ejection pressure which was so controlled as to make identification of end-systole relatively easy. (Suga et al., 1973; Suga and Sagawa, 1974; Sagawa, 1978). Consequently, the afterload imposed on the ventricle in these experiments cannot be described in terms of arterial input impedance.

There are divergent views as to the best measure of ventricular afterload. Milnor (1975) argued that arterial input impedance should best represent the afterload; Noordergraaf and Melbin (1978) argued that ventricular pressure incorporates the impedance and is more appropriate. Others consider that systolic wall tension or stress (Braunwald, 1980) should be considered the afterload. The argument on how

to define afterload has been complicated by the lack of distinction between the afterload system and the ventriculoarterial coupling variables. The afterload system for the left ventricle is the arterial input impedance which influences, but is independent of, cardiac ejection of blood into the arterial vasculature and resultant instantaneous pressure and volume of the ventricle. Because the ventricular pump interacts with its arterial load system through the systolic flow and pressure, we may consider these as the coupling variables. The wall tension or stress is a load variable on the muscle which constitutes, but should not be identified with, the ventricular load. Thus, arterial input impedance, ejection pressure, and systolic wall stress all have distinct meanings, and the one which is relevant as the afterload depends on the purpose of the study.

This study attempts to quantify the effects on the ventricular end-systolic pressure-volume relationship of changes in the parameters of the arterial input impedance. To do this, we developed simulated "physiological" preloading and afterloading systems for the isolated heart preparation (Sunagawa et al., 1982). With these systems, we could vary the afterload system parameters, i.e., resistance, capacitance, and characteristic impedance, independent of left ventricular filling. By controlling the afterload system parameters, we avoid the question as to which definition of the afterload is most appropriate.

Methods

Surgical Preparation

Twelve canine left ventricles were studied in an isolated perfused heart preparation. In each experiment, a pair of mongrel dogs was anesthetized with sodium pentobarbital (30 mg/kg, iv). The femoral arteries and veins of one dog (support dog) were cannulated and connected to a perfusion system which was used to supply oxygenated blood to the isolated heart. The perfusion system consisted of a heat exchanger, a peristaltic pump, a blood filter, and a depulsating air chamber (Fig. 1). Coronary venous blood was returned to the support dog after passing through an air trap. An oxygenator was placed in parallel to the support dog and served to support the heart during the isolation procedure and during the experiment as a backup for the support dog. The perfusion system and oxygenator were primed with one liter of 50% dextran in saline which was mixed with blood of the support dog.

The chest of the second dog (heart donor) was opened under artificial respiration. The left subclavian artery was cannulated with the arterial perfusion line of the perfusion system. The right atrium was cannulated with a tube that was connected to the return line of the perfusion system. The brachiocephalic artery was cannulated to monitor the coronary perfusion pressure. A servo system is used to drive the perfusion pump so that the coronary arterial pressure could be maintained at a constant desired level. The azygous vein, superior and inferior vena cavae, and descending aorta was ligated. The isolation of the heart was completed by ligating the lung hili. No period of interruption of coronary blood flow occurred.

The heart was removed from the donor dog and suspended over a blood collecting pan. The atrial cannula was removed and blood flowed into the collecting pan through a short Silastic vent placed in the bottom of the right ventricular lumen. A vent was also placed in the left ventricle through the apex allowing any thebesian flow to be drained. The left atrium was opened and the chordae tendinae were freed from the mitral valve leaflets. A plastic ring which served to fix the isolated heart to our volume servo pump (see below) was sutured to the mitral ring.

When the surgical preparation was complete, the isolated heart was positioned such that a water-filled balloon was inside the left ventricular (LV) cavity. Suction was applied through the LV vent so that the balloon and the LV lumen would have very nearly the same volume.

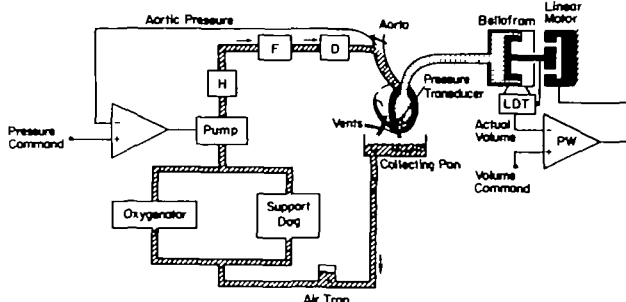


FIGURE 1. Schematic diagram of the isolated servo controlled heart preparation. H = water bath, heat exchangers, F = filter, D = debubbling chambers.

Servo-Pump Hardware

A schematic representation of the volume servo-pump system is seen in the right side of Figure 1. Details of its design and performance have previously been reported (Suga and Sagawa, 1977). Briefly, a linear motor (Ling Electronics model 411) controls the piston position of a rolling-diaphragm cylinder (Bellofram SS-4-F-SM). A latex balloon is secured to a tube connected to the fluid port of the Bellofram cylinder. The cylinder, the connecting tube, and the balloon are all filled with water. A linear displacement transducer (Trans-Tek model 244-000) senses the position of the piston, producing a signal proportional to the balloon volume. The signal is used in a negative feedback loop for comparison with a volume-command signal (see below) which represents the desired instantaneous volume. The error signal resulting from this comparison is supplied to a power amplifier (Crown DC-300), which in turn drives the linear motor.

Impedance Loading System

The volume command signal for the volume servo-system is generated by the interaction between the measured LV pressure and a specially designed hybrid computer. The details of this system were reported elsewhere (Sunagawa et al., 1982). Briefly, the left ventricular pressure, which is measured by a miniature pressure transducer (Konigsburg P-21) placed inside the balloon, serves as the input to an analog computer (Comdyna analog signal processor, model 808) which is programmed to solve the differential equations describing both the ventricular preloading and afterloading circuit illustrated in Figure 2. The two diodes in this figure, which represent the mitral and aortic valves, give rise to periods of filling and ejection and isovolumic contraction and relaxation.

The ventricular preloading model consists of a simulated constant pressure source, P_v , and a filling resistor R_f . The filling flow is calculated by dividing the pressure gradient between the pressure source and the measured pressure in the LV by R_f . Because of the presence of diode D_1 , filling occurs only when the pressure in the LV is less than P_v .

The ventricular afterloading system is the three-element WindKessel model. Flow begins when the ventricular pressure exceeds that in the simulated aorta and diode D_2 conducts. The analog computer calculates the flow by dividing the pressure difference between the measured LV pressure and P_p (see Fig. 2) by R_c . Throughout the cardiac cycle, "peripheral runoff" occurs through the resis-

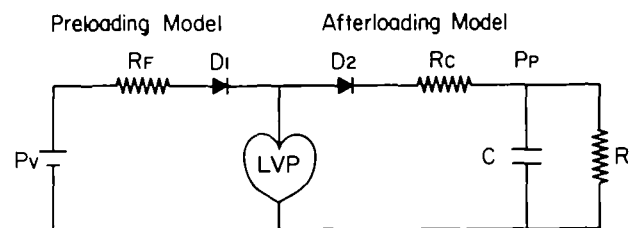


FIGURE 2. Schematic diagram of the electrical analog circuit for the vascular loading system. D_1 and D_2 are diodes representing the mitral and aortic valves and allow for an isovolumic contraction and relaxation period of the cardiac cycle. R , C , and R_c simulate the arterial resistance, capacitance, and characteristic impedance respectively. R_f models some resistance to ventricular filling. LVP in the diagram is actually measured in the isolated ejecting heart. P_p is the computed aortic pressure.

tor R . The pressure P_p is determined by the instantaneous amount of blood (charge) in the simulated arterial compliance and the magnitude of that compliance.

Both the filling and ejecting flow signals are continually integrated, and the resulting instantaneous volume signal is used as the command signal for the ventricular volume control pump. Because we are using an analog computer, the calculation of the ventricular volume changes that should result from the difference between the measured ventricular pressure and the pressure in the simulated arterial load system is instantaneous.

We have replaced all of the potentiometer controlled amplifiers of the analog computer with digital computer controlled amplifiers (Sunagawa et al., 1983). Because of this, we could accurately and reproducibly set the values of the parameters of the loading model (i.e., R_f , C , R and P_v) from the keyboard.

Cardiac output of the dog is approximately 100 ml/min per kg body weight (Guyton et al., 1973). The average weight of the heart donor dog was about 20 kg, which gives us an average cardiac output of about 30 ml/sec. The mean arterial pressure of a healthy dog is about 100 mm Hg. Therefore, the total resistance (i.e., $R_c + R$) is about 3.3 mm Hg sec/ml. Since the characteristic impedance is known to be 5–10% of the total resistance (Milnor, 1975; Nichols et al., 1980; Noble, 1979; O'Rourke and Taylor 1967; Westerhof et al., 1971, 1973), we set the normal R_c value to 0.2 mm Hg sec/ml and the R value to 3.0 mm Hg sec/ml. The time constant of decay of arterial pressure (RC in the three-element model) is about 1.1 seconds (Westerhof et al., 1971, 1973); therefore, we set the vascular compliance value at 0.4 ml/mm Hg.

Protocol

First, we obtained pressure-volume (P-V) loops at four different preloads with the parameters of the afterload impedance system set to their control values ($R_c = 0.2$ mm Hg-sec/ml, $R = 3.0$ mm Hg-sec/ml, and $C = 0.4$ ml/mm Hg). The preloads were set such that, under the control afterload condition, the highest preload would produce a peak systolic pressure of 100–120 mm Hg and the lowest preload a peak systolic pressure of about 50–60 mm Hg. The middle column in Figure 3 shows P-V loops under these control conditions. We then changed each one of the vascular parameters to half (left column in Fig. 3) and twice the control (right column in Fig. 3) and recording four P-V loops under each new afterload condition. The top row in Figure 3 shows the P-V loops under different resistances (R), the second row shows the P-V loops under different compliances (C), and the bottom row under different characteristic impedances (R_c). The ventricles were allowed to reach a steady state in 20–30 seconds at each preload and afterload condition. In order to test the stability of contractility under a given afterload condition, after obtaining four P-V loops, we set the preload back to the initial value to obtain a P-V loop. Only when the difference in the end-systolic pressures between the first loop and the test loop at the same preload was less than 10% of the initial end-systolic pressure did we accept P-V loops. Otherwise, data were discarded. Data were rejected in less than 10% of cases, and in these cases the reason for unstable contractile state was usually obvious (change in support dog condition, equipment malfunction, etc).

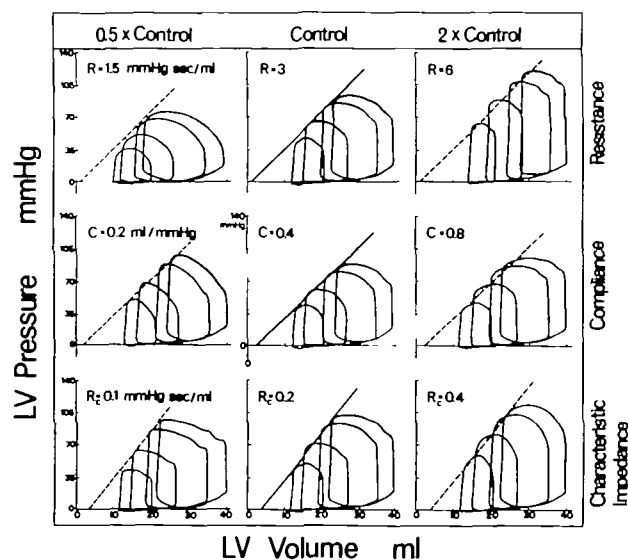


FIGURE 3. An example of the effect of interaction between the left ventricle and arterial input impedance model in one heart. Pressure-volume loops were obtained over the range from one half to twice normal resistance (top panels), compliance (middle panels), and characteristic impedance (lower panels). The panels in the center column represent P-V loops obtained under control conditions. The dashed end-systolic P-V lines in the .5X and 2X control panels are transcriptions of the end-systolic P-V relation in the control condition shown as solid lines in the center panel.

Data Analysis

We define end-systole as the instant in the cardiac cycle at which the chamber volume elastance reaches a maximum, and this instant is represented, in our view, by the upper-left corners of a set of differently preloaded pressure-volume loops (Suga et al., 1979; also see Discussion). Since our "physiologically" loaded ventricles have very rounded pressure-volume loops near end-systole, there are a number of pressure-volume points that lie on or near the ESPVR line. For the purpose of measuring the slope and intercept of the relationship line, we have found that the point of maximum pressure-volume ratio for any individual loop, although inappropriate by itself to determine the ESPVR because it ignores V_∞ , nearly always lies on or very near the "corner" of the loop. Therefore, these points with the maximum P-V ratio can be used by the computer as the initial approximation of the corner of the pressure-volume loops for the eventual determination of the ESPVR.

Thus, we first determined a pressure-volume point, at which the pressure-volume ratio became maximal on each of the four loops obtained at a given combination of afterload vascular parameters. Then we performed a least squares linear regression on these four points to obtain the slope and the volume axis intercept of the ESPVR.

Statistical Analysis

Comparisons of E_{es} and V_0 were made by a two-way analysis of variance across the three levels. Comparisons were made separately for changes in resistance and capacitance.

Results

Resistance Effect

The two left plots in Figure 4 summarize the effect of peripheral resistance change on the end-systolic P-V relationship obtained from the 12 ventricles. The slope of the ESPVR (E_{es}) did not change significantly. However, the volume axis intercept (V_o) significantly decreased with increases in the peripheral resistance, shifting the end-systolic P-V relation line towards the left. The average decrease in V_o was 4.9 ml for the increase in peripheral resistance from 50 to 200% normal.

Compliance Effect

The two middle plots in Figure 4 show the effect of vascular compliance changes on the end-systolic P-V relationship. The changes in vascular compliance did not change either the E_{es} or V_o , despite considerable changes in the shape of the P-V loop as shown in the middle row in Figure 3.

Characteristic Impedance Effect

The two righthand plots in Figure 4 show the effect of characteristic impedance changes on the ESPVR. Again, E_{es} did not change significantly. However, V_o decreased slightly but significantly. The average decrease in V_o was 1.6 ml with the increase in the characteristic impedance from 50 to 200% normal. Considering the relatively stable nature of characteristic impedance under physiological conditions, it seems reasonable to state that the practical effect of characteristic impedance changes on the ESPVR is insignificant.

Discussion

We have shown that changes in end-diastolic volume and three afterload system parameters over a wide physiological range cause a statistically significant but quantitatively small shift of the end-systolic pressure-volume relationship. Specifically,

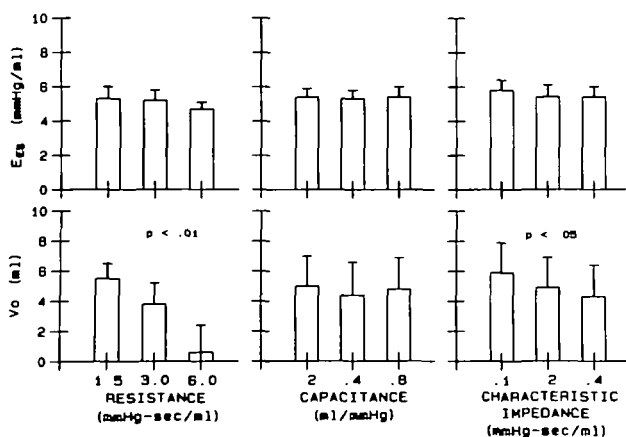


FIGURE 4. Effect of altering arterial resistance, capacitance, and characteristic impedance on the slope of the end-systolic pressure-volume relationship (E_{es}) and the volume intercept (V_o).

E_{es} does not change significantly with the change in any of the impedance system parameters, but V_o decreases slightly with increased afterload resistance and characteristic impedance.

Previously, Suga et al., 1977, 1979 used an active volume clamber in their investigation of the afterload pressure independence of E_{max} . They showed that those contractions which started from an identical end-diastolic volume and ejected to an identical end-systolic volume ended with the same end-systolic pressure, regardless of drastically different time courses of ejection pressure. However, they also showed that the end-systolic pressure increasingly deviated from that of isovolumic end-systolic pressure as the ejection fraction increased beyond 50% (Suga et al., 1979). This finding is rather consonant with the repeated observation in papillary muscle that, with increasing isotonic shortening, the force-length trajectory ends farther away from the end-systolic force-length relation curve of isometric contractions (Brady, 1967; Taylor, 1970; Suga et al., 1977). It has been suggested that the mechanism of this dependence of pressure is a deactivation effect of shortening. Besides this deactivation effect, viscoelastic properties (creep and stress relaxation) and history-dependent changes in contractile state could be involved.

The change in the ESPVR associated with changes in resistance (Fig. 3) is consistent with the observations cited above. Notice that with the subnormal resistance, the end-systolic pressure of all of the loops lie slightly below the control end-systolic P-V relation line, and with the increased resistance, the opposite tendency is present. Evidence along this line is also presented in Figure 5. The three top panels show the pressure-volume loops from one left ventricle under the same contractile state. Its end-diastolic volume was slowly decreased over 15 seconds while it was ejecting against each of three afterload resistances which were combined with normal compliance and characteristic impedance. The right top panel shows those at the high resistance. Stroke volume was small and the end-systolic P-V points lie close to a straight line. The mid top panel shows the P-V loops with a normal resistance. This end-systolic P-V relationship is very similar to that seen at the higher resistance in the high pressure range (as shown by the superposition of the ESPVRs in the bottom panel), but there is some curvilinearity in the lower pressure range. The left top panel shows that, at the low resistance, the ESPVR deviates from the other relation line. With large stroke volumes, the end-systolic pressure values are depressed in comparison to those obtained with higher resistances and smaller stroke volumes. The bottom left panel is a tracing of the ESPVRs for each of the top panels. The slight curvilinearity shown could be an explanation for the "parallel" shift of ESPVR with changed impedance parameters. In our experiments, the high resistance load was associated with P-V

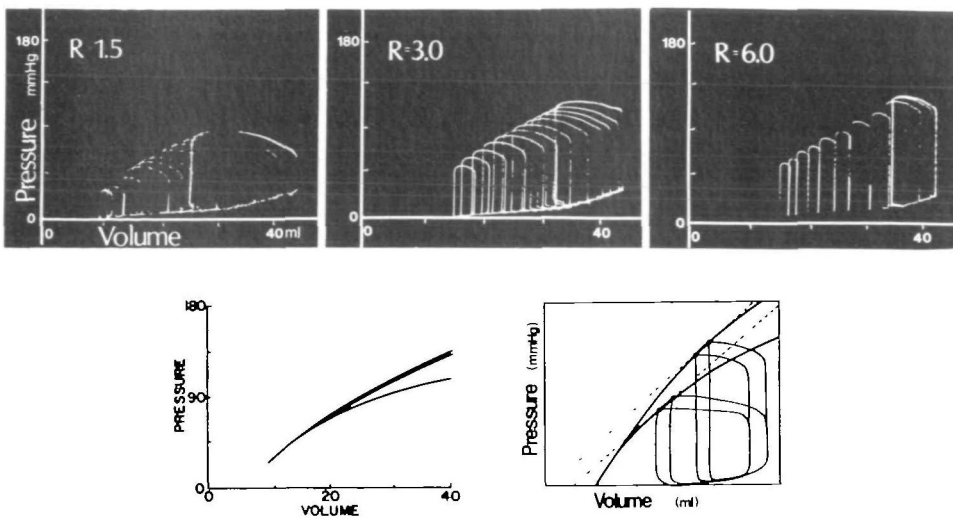


FIG. 5. Top three panels are photographs of oscilloscope tracings of pressure-volume loops obtained as preload is slowly lowered over 15 seconds. The three photos were taken at a normal resistance (3.0 mm Hg sec/ml), one half normal (1.5 mm Hg sec/ml) and twice normal (6.0 mm Hg sec/ml). The left line drawing at the bottom superimposes line tracings of the end-systolic pressure-volume relationship from each of the photographs. The right drawing is a schematic exaggeration of linear regression lines drawn from point 3 in two different loading ranges showing a parallel shift.

loops with higher end-systolic pressure than the low resistance load. The bottom right panel of Figure 5 shows a schematic drawing illustrating this point. Lines tangent to the ESPVR in the two different pressure ranges are parallel. However, arguing against stroke volume being the only determinant of this pressure deficit is the observation that at comparable stroke volumes seen with high resistance but larger end-diastolic volume and with low resistance but smaller end-diastolic volume, the end-systolic pressure deficit was often greater with the lower resistance (see Fig. 3). Therefore, ejection fraction, rather than stroke volume, may determine the pressure deficit.

Changes in the diastolic pressure-volume relationship have been shown with changes in coronary perfusion pressure (Gaasch et al., 1978). The mechanism may be related to differences in the state of filling of the large coronary vessels surrounding the myocardium (so-called garden hose effect). It is possible that the same mechanism operates at end-systole. This mechanism is unlikely to be present in our experiments in which coronary arterial pressure was held constant. It cannot be totally excluded, however, since there can be differences in the filling of small or micro coronary vessels surrounding muscle fibers.

Connecting a hydraulic impedance load similar to that developed by Westerhof et al. (1971), to canine left ventricles, Ishide et al. (1980) studied the effects on the end-systolic P-V relationship by independently changing the resistance or compliance. The resistance change experiment gave an end-systolic pressure-stroke-volume relation which was not much changed. In contrast, the results with compliance changes yielded an end-systolic pressure-stroke volume relationship curve with a vastly different slope. They concluded that the end-systolic pressure-ejected volume relationship in the ejecting heart is governed not only by contractility but also by arterial capacitance. However, to compare studies

of the "end-systolic" pressure-volume relation, any difference in definition of end-systole must be resolved or clearly recognized.

In our use of terminology, end-ejection is distinguished from end-systole (Iizuka, 1979; Suga and Nishiura, 1980; Sagawa, 1981). We use the term systole to refer to the period of actively developing contractile process independent of loading conditions. Since the beginning and end of ejection depends not only on the time course of the contractile process but also on external loading conditions, we do not use opening and closing of the aortic valve or maximum and minimum ventricular volume as the markers of onset and end of systole. Instead, we define end-systole as the instant at which the active contractile process reaches a maximum; more specifically, this is the time at which the chamber volume elastance reaches a maximum (Suga et al., 1979). Ishide et al. (1980) defined end-systole as the end of ejection, and measured end-systolic left ventricular pressure either at the end of ejection or at the time of the dicrotic notch, which usually occurs later than our end-systole. When we drew an end-systolic pressure-volume relation line tangent to the corners of their LV pressure-ejected volume loops (Fig. 5 of the paper by Ishide et al., 1980), we found almost the same slope, whether the capacitance or the resistance parameter was varied.

Elzinga and Westerhof (1981), using isolated cat trabecula contracting under a variety of afterloads found that the time for the maximum volume elastance of a hypothetical ventricle was affected by load when its pressure-volume relationship was calculated from the isolated muscle preparation based on a thin-walled cylindrical model of geometry. We also observed a similar effect of large changes in loading conditions on the time course of ventricular volume elastance change during systole. In the present study, we determined the ESPVR, not by applying regression analysis to isochronous P-V data points from differently loaded beats and finding the

maximal slope of the regression line, but by drawing a line that has a least average distance to the corners of the P-V loops.

Paulus and coworkers (1980) imposed changes in resistance and capacitance of a three-element vascular model on an isolated cat papillary muscle and examined the pressure-volume relation of a hypothetical cylindrical ventricle. They found that the ESPVR derived from changing resistance at constant preload had a lower slope and smaller intercept, compared with those derived from changing capacitance. The differences between these results and our own probably relate not only to the difference between the real ventricle and hypothetical ventricle, but also to the difference in loading patterns. In all cases, we obtained the ESPVR from several differently preloaded beats. We found this necessary, particularly with changes in capacitance and characteristic impedance, because the differences in end-systolic pressure and volume were so small over the 50–200% normal range of impedance that a reliable ESPVR could not be calculated from data obtained with afterload impedance changes alone. The end-systolic pressure changes with changed impedance and constant stroke volume seen in the Paulus model appear to be much larger than those seen in the isolated dog heart (Suga et al., 1979). We have measured the ESPVR from beats with constant preload and different afterload resistances as Paulus did, and found a slightly higher slope and larger volume intercept compared to the ESPVR of multiple preloaded beats. Since Paulus et al. did not obtain an ESPVR from beats under different preloads, we cannot directly compare their result to ours.

The isolated heart loading system used in the present experiments has the advantage of allowing continuous, highly accurate measurement of left ventricular volume and pressure while the ventricle ejects against a reasonably "physiological" afterload. Nonetheless, the afterload system used in this preparation is not a perfect model of the natural arterial system. For example, the model does not incorporate pressure wave reflection and, as a result, the impedance modulus decays smoothly toward an asymptote over the range of higher harmonics (characteristic impedance) without those oscillations which are seen in the natural arterial impedance spectrum. Although we consider this system a reasonably good representation of the hydraulic impedance characteristics of the arterial vascular network, we cannot exclude the possibility that, in the intact cardiovascular system, there might be some quantitative differences in the sensitivity of the ESPVR to changes in the dynamic properties of the arterial system. In addition, although we changed the afterload impedance parameters over a wide range (50–200% normal), it is possible that in disease states or during extreme experimental conditions, impedance changes outside this range can occur and potentially

influence the end-systolic P-V relationship to a greater extent than demonstrated here.

Although the present results show an insignificant effect of impedance changes on the slope of the ESPVR and minimal effect on the volume intercept, they also indicate the possibility of large errors when the ESPVR has to be estimated from a very limited number of pressure-volume data obtained with vasoactive agents. For instance, if a pressure-volume loop obtained under a high resistance, high preload, low ejection fraction condition (the right-most loop in the top right panel of Fig. 3) was used in combination with another P-V loop obtained under a low resistance, high ejection fraction condition (the left-most P-V loop in the left top panel of Fig. 3), the relation thus derived can produce a large overestimation of both the slope and the intercept of the ESPVR. In practice, however, we believe that the errors discussed above are usually unimportant because the loading changes used in clinical situations or intact animal preparations are ordinarily not associated with large changes in ejection fraction, but rather with simultaneous changes in preload, as well as afterloaded pressure in the same direction.

The present investigation does not provide insight into cellular mechanisms behind the observed influence of vascular impedance parameters on the ventricular ESPVR. The relationship between the P-V variables and muscle F-L variables is confounded by the complex chamber geometry, variable fiber course, asynchronous activation, and relaxation, and the resultant nonhomogeneous regional strain and stress. These confounding factors preclude precise inferences of muscle properties and mechanisms from the P-V relationship. Instead, this study was planned to be the first step to untangle the complex mechanisms behind the ventriculo-arterial system interactions in the intact circulation. As such, the excised heart and the simple three-element model were used so that we could control the experimental conditions far more exactly than is possible in the intact situation.

We know from those studies cited above that changes in the load applied to cardiac muscle influence the force-length relationship of cardiac muscle, probably by calcium-mediated change in the interaction between actin and myosin. In addition, it seems likely that large changes in afterload lead to changes in ventricular geometry with a redistribution of regional wall stresses, and also lead to differences in coronary blood flow and blood flow distribution as well as regional differences in metabolic demand. Furthermore, there may be changes in the activation sequence and conduction times. With the multiplicity of factors which may be associated with afterload changes, it is surprising that even larger changes were not seen in the ESPVR relative to the small changes observed in this study.

The physiological significance of the present findings can be considered with respect to stroke volume

and stroke work of the left ventricle. Several investigators (O'Rourke, 1967; Milnor, 1975; Nichols et al., 1977) have measured changes in the characteristic impedance with heart disease, exercise, and drugs in man (Nichols et al., 1977, 1980; Pepine et al., 1978) or animals (O'Rourke, 1967; Pouleur et al., 1979) and some of them presumed that these changes, ranging from -50 to +200% in magnitude, may have important effects on ventricular stroke volume. The present findings of a very small horizontal shift of the ESPVR (V_0 shift of 1.6 ml) with a similar magnitude of characteristic impedance change, cast serious doubt on that concept. If the in vivo heart behaves like our excised hearts, the direct mechanical effect of a change in characteristic impedance on stroke volumes of those beats which begin with an identical end-diastolic volume, and end under an identical end-systolic pressure, will be only 1.6 ml. In a 20-kg conscious dog with a normal stroke volume of 25 ± 5 ml, the effect is only about 6%. This is perhaps within the measurement error range. Therefore, further quantitative validation is warranted of the concept that changes in characteristic impedance in the observed range of magnitude is important for stroke volume.

On the other hand, the 50–200% change in peripheral resistant horizontally shifted the ESPVR by about 5 ml. This corresponds to 16–25% of the normal stroke volume assumed above. This is not a negligible amount. The pathophysiological effect of this finding is that the increase in stroke volume by afterload resistance reduction will be slightly less than what is expected with unaltered ESPVR. Note, however, that the attenuation will not be quite as large as the change in V_0 measured in this study because mean and end-systolic aortic pressure will decrease, and this lower end-systolic pressure will in turn augment the stroke volume. The eventual net attenuation will therefore be less than the change in V_0 's. A more accurate prediction can be made using Equations 9 and 10 of our previous paper (Sunagawa et al., 1983).

In a recent analysis of the interaction between the left ventricle and arterial impedance (Sunagawa et al., 1983), we made theoretical prediction of stroke volume under a control set of arterial impedance parameters similar to the present set and then by coupling the ESPVR with non-control sets of arterial impedance. That is, when the peripheral resistance parameter was altered over a wide range, we did shift the ESPVR left or right by the amount of change in V_0 reported here. Nonetheless, the predicted stroke volume values correlated with the actual afterload with a regression coefficient of 1.00 ± 0.04 , and intercept of 1.0 ± 0.2 and a correlation coefficient of 0.985 ± 0.004 . This nearly perfect prediction is strong additional evidence that the horizontal shifts of the ESPVR reported here have a relatively small effect on stroke volume.

In conclusion, in isolated canine left ventricles

perfused with constant coronary pressure the slope end-systolic pressure-volume relationship is insensitive to changes in afterload system parameters such as arterial resistance, capacitance, and characteristic impedance, whereas the volume intercept can be mildly influenced by large changes in resistance and characteristic impedance.

Supported by U.S. Public Health Service Research Grant HL-14903 and Ischemic Disease SCOR HL-17655.

Address for reprints: W. Lowell Maughan, M.D., Carnegie 592, Cardiology Division, Department of Medicine, Johns Hopkins Hospital, 600 North Wolfe Street, Baltimore, Maryland 21205.

Received December 17, 1982; accepted for publication March 13, 1984.

References

- Brady H (1967) Length-tension relations compared in cardiac muscle. *Am Zoologists* 7: 603–610
- Braunwald E (1980) Heart disease. In *A Textbook of Cardiovascular Medicine*, Philadelphia, W.B. Saunders Company, pp 438–439
- Elzinga G, Westerhof N (1981) "Pressure-volume" relations in isolated cat trabecula. *Circ Res* 49: 388–394
- Gaasch WH, Bing OHL, Franklin A, Rhodes D, Bernard SA, Weintraub RM (1978) The influence of acute alterations in coronary blood flow on left ventricular diastolic compliance and wall thickness. *Eur J Cardiol* 7 (suppl): 147–161
- Guyton GC, Jones CE, Coleman TG (1973) Normal cardiac output and its variations. In *Circulatory Physiology: Cardiac Output and Its Regulation* ed 2, Philadelphia, Saunders, pp 3–20
- Iizuka M (1979) Comments on "The Ventricular Pressure-Volume Diagram Revisited." *Circ Res* 44: 731
- Ishide N, Shimizu Y, Maruyama Y, Koiwa Y, Nunokawa T, Isoyama S, Kotaoka S, Tamaki T, Inooka E, Takishima T (1980) Effects of changes in the aortic input impedance on systolic pressure-ejected volume relationships in the isolated supported canine left ventricle. *Cardiovasc Res* 14: 229–243
- Marsh JD, Green LH, Wynne J, Cohn PF, Grossman W (1979) Left ventricular end-systolic pressure-dimension and stress-length relations in normal human subjects. *Am J Cardiol* 44: 1311–1317
- Mehmel H, Stockins B, Ruffmann K, Olshausen K, Schuler G, Kubler W (1981) The linearity of the end-systolic pressure-volume relationship in man and its sensitivity for assessment of left ventricular function. *Circulation* 63: 1216–1222
- Milnor WR (1975) Arterial impedance as ventricular afterload. *Circ Res* 36: 565–570
- Nichols WW, Conti CR, Walker WE, Milnor WR (1977) Input impedance of the systemic circulation in man. *Circ Res* 40: 451–458
- Nichols WW, Pepine CJ, Geiser EA, Conti R (1980) Vascular load defined by the aortic input impedance spectrum. *Fed Proc* 39: 196–201
- Nivatpumin T, Katz S, Scheur J (1979) Peak left ventricular systolic pressure/end-systolic volume ratio: A sensitive detector of left ventricular disease. *Am J Cardiol* 43: 969–974
- Noble MM (1979) Left ventricular load, arterial impedance and their interrelationship. *Cardiovasc Res* 13: 183–198
- Noordergraaf A, Melbin J (1978) Ventricular afterload: a succinct yet comprehensive definition. *Am Heart J* 95: 545–547
- O'Rourke MF (1967) Steady and pulsatile energy losses in the systemic circulation under normal conditions and in simulated arterial disease. *Cardiovasc Res* 1: 313–326
- O'Rourke MF, Taylor MG (1967) Input impedance of the systemic circulation. *Circ Res* 20: 365–380
- Paulus WJ, Claes VA, Brutsaert DL (1980) End-systolic pressure-volume relation estimated from physiologically loaded cat papillary muscle contractions. *Circ Res* 46: 20–26

- Pepine CJ, Nichols WW, Conti CR (1978) Aortic input impedance in heart failure. *Circulation* **58**: 460-465
- Pouleur H, Covell JW, Ross J Jr (1979) Effects of alterations in aortic input impedance on the force-velocity-length relationship in the intact canine heart. *Circ Res* **45**: 126-135
- Sagawa K (1978) The ventricular pressure-volume diagram revisited. *Circ Res* **43**: 677-687
- Sagawa K (1979) Reply to Comments on "The ventricular pressure-volume diagram revisited." *Circ Res* **44**: 731
- Sagawa K (1981) Editorial: The end-systolic pressure-volume relation of the ventricle: Definition, modifications and clinical use. *Circulation* **63**: 1223-1227
- Sagawa K, Suga H, Shoukas A, Bakalar K (1977) End-systolic pressure/volume ratio: A new index of ventricular contractility. *Am J Cardiol* **40**: 748-753
- Suga H, Nishiura N (1980) Dissociation of end ejection from end systole of ventricle. *Jpn Heart J* **22**: 117-125
- Suga H, Sagawa K (1974) Instantaneous pressure-volume relationships and their ratio in the excised supported canine left ventricle. *Circ Res* **35**: 117-126
- Suga H, Sagawa K (1977) End-diastolic and end-systolic ventricular volume clamber for isolated canine heart. *Am J Physiol* **233**: H718-H722
- Suga H, Yamakoshi K (1977) Effects of stroke volume and velocity of ejection on end-systolic pressure of canine left ventricle. *Circ Res* **40**: 445-450
- Suga H, Sagawa K, Shoukas A (1973) Load independence of the instantaneous pressure-volume ratio of the canine left ventricle and effects of epinephrine and heart rate on the ratio. *Circ Res* **32**: 314-322
- Suga H, Saeki T, Sagawa K (1977) End-systolic force-length relationship of non-excised canine papillary muscle. *Am J Physiol* **233**: H711-H717
- Suga H, Kitabatake A, Sagawa K (1979) End-systolic pressure determines stroke volume from fixed end-diastolic volume in the isolated canine left ventricle under a constant contractile state. *Circ Res* **44**: 238-249
- Sunagawa K, Burkhoff D, Lim K, Sagawa K (1982) Impedance loading servo pump system for excised canine ventricle. *Am J Physiol* **243**: H346-H350
- Sunagawa K, Lim KO, Burkhoff D, Sagawa K (1983) Microprocessor control of a ventricular volume servo-pump. *Ann Biomed Eng* **10**: 145-159
- Sunagawa K, Maughan WL, Burkhoff D, Sagawa K (1983) Left ventricular interaction with arterial load studied in isolated canine ventricle. *Am J Physiol* **245**: 773-780
- Taylor R (1970) Active length-tension relations compared in isometric afterload and isotonic contractions of cat papillary muscle. *Circ Res* **26**: 279-288
- Westerhof N, Elzinga G, Sipkema P (1971) An artificial arterial system for pumping hearts. *J Appl Physiol* **36**: 123-127
- Westerhof N, Elzinga G, Van Den Bos GC (1973) Influence of central and peripheral changes on the hydraulic input impedance of the systemic arterial tree. *Med Biol Eng* **11**: 710-723

INDEX TERMS: Excised canine heart • Isolated left ventricle • Left ventricular pump function • Arterial resistance • Arterial compliance • Arterial characteristic impedance